Analyst

PAPER

View Article Online
View Journal | View Issue

Cite this: *Analyst*, 2015, **140**, 1215

Multiplexed detection of two proteins by a reaction kinetics-resolved chemiluminescence immunoassay strategy

Wenwen Wang, Hui Ouyang, Shijia Yang, Lin Wang* and Zhifeng Fu*

A multiplexed immunoassay method was proposed for the sequential detection of two proteins in a single run based on a novel chemiluminescence (CL) reaction kinetics-resolved strategy. This method was established using acridinium ester (AE) and alkaline phosphatase (ALP) as the signal probes due to the significant difference in their CL reaction kinetics characteristics. Mouse IgG (MIgG) and mouse IgM (MIgM) were detected as the model analytes with a competitive immunoassay format. AE and ALP were used to tag goat anti-mouse IgG and rabbit anti-mouse IgM, respectively, to form two immunocomplexes. The two CL reactions with flash type and glow type kinetics characteristics were triggered simultaneously by adding the coreactants, then the CL signals from the two reactions were recorded after 0.2 s and 500 s of the reaction triggering, respectively. The multiplexed CL immunoassay provided a wide range of 0.50–200 ng mL^{-1}, with a low detection limit of 0.16 ng mL^{-1} (S/N = 3) for both MIgG and MIgM. Additionally, no obvious signal overlap was observed in the multiplexed immunoassay. The proposed method was successfully applied for the detection of MIgG and MIgM levels in mouse serums, and the results were in good agreement with those from the reference ELISA method. We anticipate that it can be used in some other areas such as drug screening, food safety, environment monitoring and clinical diagnosis.

Received 21st October 2014,
Accepted 4th December 2014

DOI: 10.1039/c4an01921k

www.rsc.org/analyst

1. Introduction

There is increasing interest in developing multiplexed immunoassays that can substitute parallel single-analyte immunoassays in clinical diagnosis, environmental monitoring, and biodefense applications.[1] A multiplexed immunoassay shows some unique advantages, such as less sample consumption, shorter assay time, minimized repetitions of tedious procedures, and lower cost per test, in comparison with the conventional parallel single analyte detection. Moreover, it is convenient for the analysis of some complex real samples, such as biological or environmental samples, in which many different analytes can interfere with the signal of a specific sensor.[2]

Nowadays, array mode and multi-label mode have been widely utilized in a multiplexed immunoassay.[3] For the array mode, a universal signal probe is usually utilized to tag all analytes for fluorescence,[4] colorimetric,[5] chemiluminescence (CL),[6–8] electrochemical[9–11] or surface-enhanced Raman spectroscopic[12] detection. These methods sometimes encounter signal cross-talk between the adjacent detection zones resulting from the diffusion of the active product.[13] When the multi-label mode is employed, multiple signal probes are used to tag different antibodies or antigens corresponding to the analytes (one per analyte), in which the labels include enzymes,[14,15] metal ions,[16] fluorescent dyes[17] and nanoparticles.[18,19] For this mode wavelength[15,17,19] and potential[14,18] are usually utilized to distinguish the signal of one label from the others. However, such multi-label based multiplexed immunoassays are often limited by the overlap of signals from different labels due to their broad signal band.[20] In view of the above, it is still a challenge to construct multiplexed immunoassays free of signal overlap based on the multi-label mode.

Compared with the other multiplexed immunoassays, the chemiluminescence immunoassay (CLIA) has shown great potential in terms of its low background and wide linear range. Furthermore, CL detection is usually conducted on simple and inexpensive instrumentation without an external light source and optical splitting system,[21] which facilitates developing a point-of-care diagnosis method using a portable detector. Differing from the fluorometric and spectrophotometric approach, CL intensity is the only considered factor in a CL assay, while wavelength is not considered, thus, it is very difficult to distinguish CL signals from different labels.[22]

Key Laboratory of Luminescence and Real-Time Analytical Chemistry (Ministry of Education), College of Pharmaceutical Sciences, Southwest University, Chongqing 400716, China. E-mail: fuzf@swu.edu.cn; Fax: +86 23 6825 1048; Tel: +86 23 6825 0184

Therefore, multiplexed CL detection is commonly established based on array mode.[6–8]

Up to now, most CL systems can be classified into three categories based on their different reaction kinetics characteristics. The first category is the flash type showing a short-lived (seconds) but intense signal, including a heavy metal ion-catalyzed luminol-H_2O_2 system[23] and an acridinium ester (AE)-H_2O_2 system;[24,25] the second category is the glow type indicating a longer-lived (minutes to hours) and continuous increasing CL emission, such as the alkaline phosphatase (ALP)-adamantyl-1,2-dioxetane system;[26] and the third category is the oscillating type whose CL signals periodically grow and decay, such as the $Ru(bpy)_3^{2+}$-catalyzed Belousov–Zhabotinsky system.[27] The quite distinct kinetics characteristics of these CL reactions provide a possible pathway to detect multiple analytes in a single run with a reaction kinetics resolution strategy. CL reactions show a wide time window ranging from seconds to hours, thus a discrimination of signals from different probes can be easily achieved with the aid of a regular timer. However, for a time-resolved fluorescence assay which also collects signals from different fluorophores at different time windows, a sophisticated timing instrumentation is required since the lifetime of most fluorophores typically ranges from the ps to ms level.[20,28,29]

As a typical flash-type CL substance with an emission duration of 0.2 s, AE has been employed in immunoassays because of its high CL efficiency.[30] ALP-adamantyl-1,2-dioxetane reaction is a glow type CL system with a signal increasing duration of hours, accomplished with a distinguished sensitivity.[26] In this research, a novel reaction kinetics-resolved multiplexed detection strategy was developed using AE and ALP as the CL labels in the immunoassay. Mouse IgG (MIgG) and mouse IgM (MIgM) were detected as the model analytes with a competitive format. After the coreactants were added, the two different CL reactions were triggered simultaneously. However, due to the significant difference in the reaction kinetics characteristics of the labels, the two CL signals were collected at different time windows.

2. Experimental

2.1 Materials and equipments

MIgG, MIgM, mouse IgA (MIgA), polyclonal goat anti-mouse IgG, and ALP-tagged rabbit anti-mouse IgM were all purchased from Beijing Biosynthesis Biotechnology Co., Ltd (China). Mouse serum albumin (MSA) and mouse prealbumin (MPA) were purchased from Shanghai Jiahe Biotechnology Co., Ltd (China). AE labeling kit was provided by Enzo Life Sciences, Inc. (USA), and AE tagging of goat anti-mouse IgG was performed according to the manual. The ELISA kits for MIgG and MIgM were provided by Chongqing Biospes Co., Ltd (China). Healthy adult Kunming mice were obtained from Chongqing Tengxin Biotechnology Co., Ltd (China). Blood samples were obtained from the eyeballs of the mice, and centrifuged at 3000 rpm for 20 min to obtain the sera. The ALP substrate solution composed of disodium 3-(4-methoxy-spiro{1,2-dioxetane-3,2′-(5′-chloro) tricyclo [3.3.1.1^{3,7}]decan}-4-yl) phenyl phosphate (CSPD, a derivative of adamantyl-1,2-dioxetane compound) and Sapphire-IITM enhancer were purchased from Boson Biotech. Co., Ltd (China). SuperBlock® T20 (Thermo Fisher Scientific Inc., USA) was utilized as the blocking buffer. The coating buffer was 0.10 M Tris-HCl at pH 8.0. The dilution buffer for the antibodies, antigens and tracers was 0.10 M Tris-HCl at pH 7.2. The wash buffer was 0.10 M Tris-HCl at pH 7.4, containing 0.05% Tween-20. All aqueous solutions were prepared using ultrapure water (18.2 MΩ) produced by an ELGA PURELAB Classic system (UK). All other reagents were of analytical reagent grade and used without further purification.

The polystyrene high-affinity 96-well microplate was provided by Greiner Bio-One Biochemical Co., Ltd (Germany). All CL measurements were performed using an MPI-A CL analyzer (Xi'an Remax Electronic Science & Technology Co., Ltd, China) equipped with a photomultiplier operated at −800 V.

2.2 Procedure of competitive CLIA

Each well of the polystyrene microplate was coated at 4 °C for 12 h with 100 μL of a mixture of MIgG (20 μL mL^{-1}) and MIgM (10 μL mL^{-1}) dissolved in the coating buffer. Subsequently, the well was washed thrice with 260 μL of the wash buffer manually and blocked with 150 μL of the blocking buffer for 90 min at 37 °C. After that, the well was washed thrice and filled with 80 μL of the sample solution containing MIgG and MIgM at different concentrations, followed by a mixture of AE-tagged goat anti-mouse IgG and ALP-tagged rabbit anti-mouse IgM (10 μL for each). The competitive immune reactions were allowed to last for 90 min at 37 °C. Then the microplate was washed to remove the unbound reactants.

The CL reactions were triggered by adding 60 μL of the freshly prepared coreactants composed of H_2O_2 and ALP substrate in a carbonate buffer saline (CBS). The CL signals for MIgG and MIgM were detected at 0.2 s and 500 s after the reactions were triggered, respectively.

3. Results and discussion

3.1 The principle of reaction kinetics-resolved CL for multiplexed detection

The principle of reaction kinetics-resolved CL strategy for the multiplexed detection of MIgG and MIgM is illustrated in Fig. 1. AE and ALP were adopted as the flash type and glow type CL probes to tag goat anti-mouse IgG and rabbit anti-mouse IgM, respectively. Then the AE- and ALP-tagged immunocomplexes were formed in a competitive immunoassay format. Since the two tagged probes showed very different kinetics characteristics, the signals from the different analytes could be sequentially collected in different time windows after the two CL reactions were triggered simultaneously.

To demonstrate the feasibility of this reaction kinetics-resolved strategy, the kinetics behaviors of the two CL systems were investigated in detail. Fig. 2A presents the individual kinetics curves of the two CL reactions. As shown in this figure, CL emission from the AE-H_2O_2 system increased

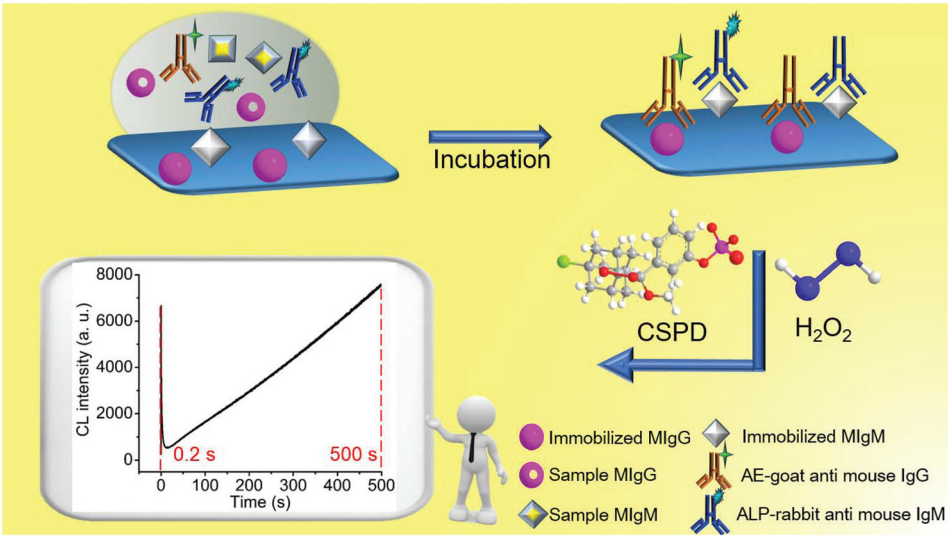

Fig. 1 Schematic illustration of the reaction kinetics-resolved CLIA for the multiplexed detection of MIgG and MIgM.

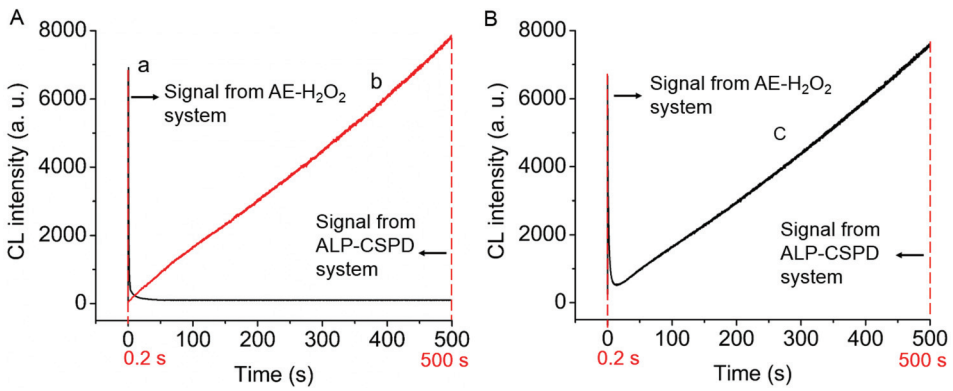

Fig. 2 (A) The CL kinetics curves of (a) the AE-H_2O_2 reaction alone for MIgG (0.5 ng mL^{-1}) detection and (b) the ALP-CSPD reaction alone for MIgM (0.5 ng mL^{-1}) detection. (B) The CL response curve of (c) the mixed CL reactions for MIgG (0.5 ng mL^{-1}) and MIgM (0.5 ng mL^{-1}) detection. All other conditions were optimal.

sharply to the maximum at about 0.2 s after the coreactants were added, and then decayed quickly within 10 s (curve a). However, the CL emission from the ALP-CSPD system was very weak within 10 s of reaction triggering, then increased continuously and steadily in a long duration (curve b). Fig. 2B shows the CL kinetics curve (curve c) of the mixed reaction system of AE-H_2O_2 and ALP-CSPD. As shown in this figure, the flash type reaction of the AE-H_2O_2 system was not obviously affected by the glow type one. However, for the glow type reaction of the ALP-CSPD system, the signal from this CL reaction was found to be obviously affected by the co-existing AE-based CL system at the beginning of the reaction triggering. After 70 s, the CL kinetics curve of the ALP-catalyzed reaction in the mixed system overlapped with that in the individual system, which indicated that the mutual influence was avoided effectively after 70 s.

As shown in Fig. 1, MIgG was detected at 0.2 s since the AE-H_2O_2 system showed the maximal emission at this time. For MIgM detection, the ALP-CSPD system showing a continuously increased signal was adopted, thus the long reaction time resulted in an obviously improved signal intensity and detection sensitivity, for example, signals for 100 ng mL^{-1} MIgM at 700 s and 1000 s showed an increase of 38% and 101%, respectively, in comparison with that at 500 s. However, the long signal acquisition time led to a low assay speed. The five hundredth second was chosen as the time window for MIgM signal detection considering the assay speed. Obviously, at the chosen time windows, the two CL reactions did not show any observable mutual interference. Therefore, a multiplexed CLIA can be easily achieved without using any optical splitting system for wavelength discrimination.

3.2 Optimization of CLIA conditions

The performance of an immunoassay usually depends on such parameters as the concentrations of the tracer antibodies and the incubation time. The effects of the concentrations of the

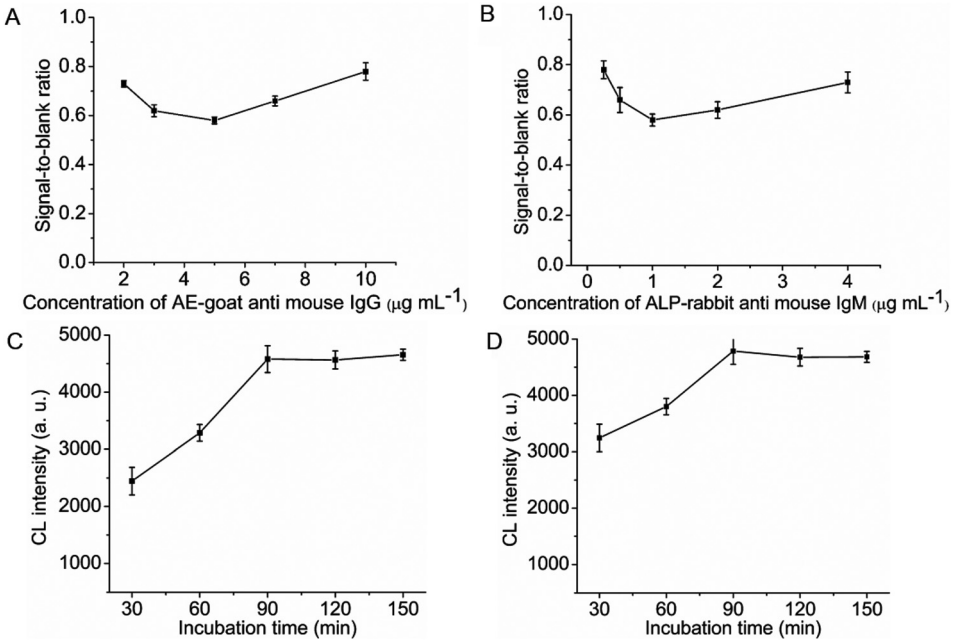

Fig. 3 Effects of the concentrations of the tracer antibodies on their corresponding signal-blank-ratios for (A) MIgG and (B) MIgM at 100 ng mL^{-1}. Effects of the incubation times on the CL responses for (C) MIgG and (D) MIgM at 100 ng mL^{-1}. All other conditions were optimal, n = 5.

tracer antibodies on the CL responses were investigated using MIgG (100 ng mL^{-1}), MIgM (100 ng mL^{-1}) and Tris-HCl (as a blank) in parallel. Fig. 3A and B show that the signal-to-blank ratios reached the minimum when the concentrations of the tracer antibodies for MIgG and MIgM were 5.0 μg mL^{-1} and 1.0 μg mL^{-1}, respectively, indicating that the competition capability of the two analytes in the sample against the immobilized antigens was the strongest under these conditions. The effect of the incubation time on the immunoreactions was also studied in detail. From Fig. 3C and D, it was found that both the CL responses almost trended the maximum at 90 min, suggesting that the immuno-binding reached the saturation at this incubation time. Therefore, the concentrations of 5.0 μg mL^{-1} and 1.0 μg mL^{-1} for the tracer antibodies for MIgG and MIgM, respectively, and the incubation time of 90 min were adopted in the further investigation.

For CL detection, the pH value and the concentrations of the coreactants were the crucial factors influencing the signal intensities and the reaction kinetics characteristics. The optimal pH values for the AE-H_2O_2 and ALP-CSPD systems were around 13.0[31–33] and 9.5,[26] respectively. High pH value was found to damage the activity of ALP, thus inhibiting CL emission from the ALP-CSPD system. Meanwhile, AE-H_2O_2 emitted a strong CL signal only in a strong basic medium. Thus, a compromised pH value of 11.6 was adopted since both the reaction systems showed acceptable signal intensity and detection sensitivity. Also, the pH value showed a noticeable influence to the reaction kinetics characteristics of both the CL reactions, and therefore affected the signal resolution. An ideal signal resolution was obtained at this compromised pH value. For the same reason, the optimal concentrations of

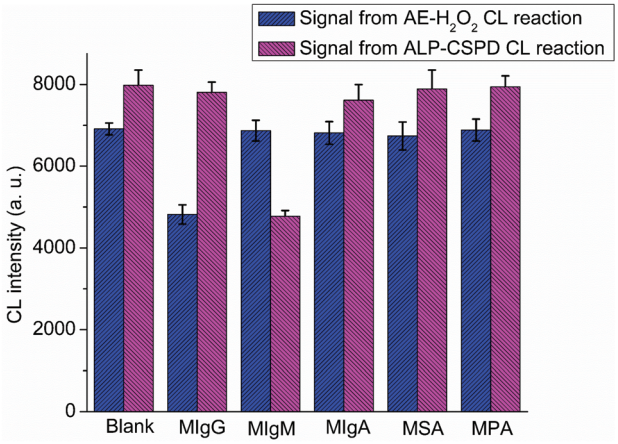

Fig. 4 The CL responses of MIgG, MIgM, MIgA, MSA, and MPA at 100 ng mL^{-1}. The Tris-HCl buffer was used as the blank. All other conditions were optimal, n = 5.

H_2O_2, CSPD and Sapphire-IITM enhancer were chosen to be 20 mM, 67 mM and 0.33 mg mL^{-1}, respectively.

3.3 Estimation of specificity

In order to evaluate the specificity of this immunoassay method, the interferences of various species including MIgA, MSA and MPA were investigated since these proteins exist in the real mouse serum samples. The specificity was estimated by comparing the responses to MIgG, MIgM and the interferent proteins. As shown in Fig. 4, an obvious decrease of 30% and 40% in the CL intensity was observed for MIgG and MIgM at 100 ng mL^{-1}, respectively, since a competitive format was adopted in this method, while MIgA, MSA and MPA at the

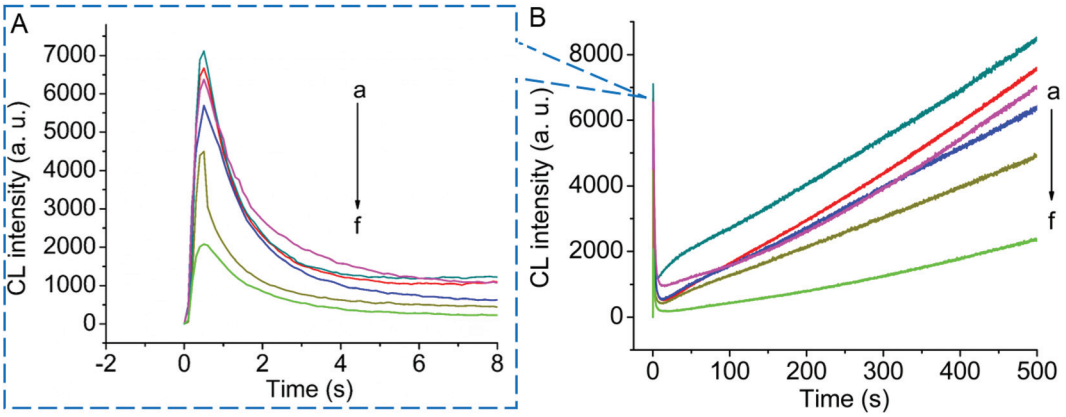

Fig. 5 (A) An enlarged view of the CL responses of MIgG. (B) The CL responses of MIgG and MIgM at the concentrations of (a) 0, (b) 0.5, (c) 25, (d) 50, (e) 100, and (f) 200 ng mL^{-1}. All other conditions were optimal, n = 5.

same concentration showed a negligible decrease below 4.6%. The results suggested that the specificity of the multiplexed detection method for MIgG and MIgM was acceptable for a real sample assay.

3.4 Performance of CLIA

As shown in Fig. 5, under optimal conditions, the CL responses decreased linearly with the increasing concentrations of MIgG and MIgM since a competitive immunoassay format was adopted. The linear range was 0.50–200 ng mL^{-1}, with a detection limit of 0.16 ng mL^{-1} at a signal to noise ratio of 3, for both MIgG and MIgM. The regression equations could be expressed as I (a. u.) = $-23.3C$ (ng mL^{-1}) + 6837 and I (a. u.) = $-26.1C$ (ng mL^{-1}) + 7543, with the correlation coefficients of 0.9915 and 0.9818 for MIgG and MIgM, respectively. The reproducibility was assessed by intra- and inter-day relative standard deviations (RSDs) for MIgG and MIgM at low (0.5 ng mL^{-1}) and high (100 ng mL^{-1}) concentrations. As shown in Table 1, the intra- and inter-day RSDs were not higher than 4.5 and 4.9%, respectively.

Table 1 Reproducibility for MIgG and MIgM detection (n = 5)

Analyte	MIgG		MIgM	
Concentration (ng mL^{-1})	0.5	100	0.5	100
Intra-day RSD (%)	1.0	4.5	2.2	4.0
Inter-day RSD (%)	1.1	4.9	3.3	4.7

Table 2 Assay results of the mouse serum samples using the proposed and reference methods (n = 5)

	Concentration of MIgG (mg mL^{-1})		Concentration of MIgM (mg mL^{-1})	
Sample no.	Proposed method[a]	ELISA[b]	Proposed method[a]	ELISA[b]
1	8.1 ± 0.3	8.4 ± 0.1	0.25 ± 0.07	0.25 ± 0.03
2	6.8 ± 0.1	7.3 ± 0.3	0.22 ± 0.08	0.21 ± 0.01
3	6.4 ± 0.7	6.7 ± 0.2	0.28 ± 0.08	0.26 ± 0.05

[a] The samples were 2 × 10^5-time diluted. [b] The samples were 100-time diluted.

3.5 Application in the real sample assay

In order to further estimate the application potential of this CL reaction kinetics-resolved strategy, the levels of MIgG and MIgM in three healthy adult mouse serum samples were evaluated with this method, and the obtained results were compared with those from the reference ELISA method. All samples were diluted before assay to ensure that the concentrations were within the linear ranges. From Table 2, it can be seen that the two methods showed acceptable agreement. Known amounts of MIgG and MIgM were spiked into the diluted samples to perform the recovery tests. The recoveries for MIgG and MIgM were 88.0–109.6% and 90.0–112.0%, respectively, demonstrating the reliability of this method (Table 3).

Table 3 The results of the recovery tests of MIgG and MIgM spiked in the mouse serum samples obtained by the proposed method (n = 5)

	1		2		3	
Sample no.[a]	MIgG	MIgM	MIgG	MIgM	MIgG	MIgM
Initial (ng mL^{-1})	40.5	1.2	34.0	1.1	32.0	1.4
Added (ng mL^{-1})	10.0	1.0	25.0	2.5	50.0	5.0
Found (ng mL^{-1})	49.3 ± 2.9	2.1 ± 0.1	61.4 ± 1.9	3.7 ± 0.3	82.2 ± 1.1	7.0 ± 0.6
Recovery (%)	88.0	90.0	109.6	104.0	100.4	112.0

[a] Mouse serum samples were 2 × 10^5-time diluted prior to the recovery test.

4. Conclusions

In summary, a novel CL reaction kinetics-resolved strategy was designed for a multiplexed immunoassay using AE and ALP as the labels. This strategy did not need an optical splitting system to distinguish the signals from the two CL probes. Due to the very different reaction kinetics characteristics of the two CL probes (a flash type and a glow type), MIgG and MIgM could be sequentially detected in different time windows with the aid of a regular timer. This proposed method was simple, rapid and low-cost. Furthermore, no signal overlapping was found in this work, which was frequently encountered in the previously reported multiplexed immunoassays based on the multi-label mode. The results of the real sample assay and the recovery test demonstrated its reliability and application potential. Further work utilizing more CL labels to detect more analytes in a single run is still ongoing. We anticipate that this multiplexed detection method can be used in some important areas such as drug screening, food safety and clinical diagnosis.

Acknowledgements

This project was financially supported by the Natural Science Foundation of China (21175111 and 21475107), the Natural Science Foundation of Chongqing (CSTC2013jjB0096), the Fundamental Research Funds for the Central Universities (XDJK2013A025, XDJK2014C088 and 2362014xk07), and the Program for Innovative Research Team in the University of Chongqing (2013).

Notes and references

1 Y. Zhou, Y. H. Zhang, C. W. Lau and J. Z. Lu, *Anal. Chem.*, 2006, **78**, 5920–5924.
2 S. Carregal-Romero, E. Caballero-Díaz, L. Beqa, A. M. Abdelmonem, M. Ochs, D. Hühn, B. S. Suau, M. Valcarcel and W. J. Parak, *Annu. Rev. Anal. Chem.*, 2013, **6**, 53–81.
3 Z. H. Yang, Y. Zhuo, Y. Q. Chai and R. Yuan, *Sci. Rep.*, 2014, **4**, 4747.
4 S. H. Kim, J. W. Shim and S. M. Yang, *Angew. Chem., Int. Ed.*, 2011, **50**, 1171–1174.
5 P. Novo, D. M. F. Prazeres, V. Chu and J. P. Conde, *Lab Chip*, 2011, **11**, 4063–4071.
6 C. Zong, J. Wu, J. Xu, H. X. Ju and F. Yan, *Biosens. Bioelectron.*, 2013, **43**, 372–378.
7 A. Roda, M. Mirasoli, L. S. Dolci, A. Buragina, F. Bonvicini, P. Simoni and M. Guardigli, *Anal. Chem.*, 2011, **83**, 3178–3185.
8 S. M. Wang, L. Ge, X. R. Song, J. H. Yu, S. G. Ge, J. D. Huang and F. Zeng, *Biosens. Bioelectron.*, 2012, **31**, 212–218.
9 L. Ge, J. X. Yan, X. R. Song, M. Yan, S. G. Ge and J. H. Yu, *Biomaterials*, 2012, **33**, 1024–1031.
10 M. S. Wu, H. W. Shi, L. J. He, J. J. Xu and H. Y. Chen, *Anal. Chem.*, 2012, **84**, 4207–4213.
11 F. Y. Kong, B. Y. Xu, Y. Du, J. J. Xu and H. Y. Chen, *Chem. Commun.*, 2013, **49**, 1052–1054.
12 Z. Chen, S. M. Tabakman, A. P. Goodwin, M. G. Kattah, D. Daranciang, X. R. Wang, G. Y. Zhang, X. L. Li, Z. Liu, P. J. Utz, K. L. Jiang, S. S. Fan and H. J. Dai, *Nat. Biotechnol.*, 2008, **26**, 1285–1292.
13 G. S. Lai, L. L. Wang, J. Wu, H. X. Ju and F. Yan, *Anal. Chim. Acta*, 2012, **721**, 1–6.
14 K. Dill, A. Ghindilis and K. Schwarzkopf, *Lab Chip*, 2006, **6**, 1052–1055.
15 Y. X. Piao, D. Lee, J. Lee, T. Hyeon, J. Kim and H. S. Kim, *Biosens. Bioelectron.*, 2009, **25**, 906–912.
16 S. H. Hu, S. C. Zhang, Z. C. Hu, Z. Xing and X. R. Zhang, *Anal. Chem.*, 2007, **79**, 923–929.
17 E. Barash, S. Dinn, C. Sevinsky and F. Ginty, *IEEE Trans. Med. Imaging*, 2010, **29**, 1457–1462.
18 J. Qian, H. C. Dai, X. H. Pan and S. Q. Liu, *Biosens. Bioelectron.*, 2011, **28**, 314–319.
19 L. Chen, X. W. Zhang, G. H. Zhou, X. Xiang, X. H. Ji, Z. H. Zheng, Z. K. He and H. Z. Wang, *Anal. Chem.*, 2012, **84**, 3200–3207.
20 Y. Q. Lu, J. B. Zhao, R. Zhang, Y. J. Liu, D. M. Liu, E. M. Goldys, X. S. Yang, P. Xi, A. Sunna, J. Lu, Y. Shi, R. C. Leif, Y. J. Huo, J. Shen, J. A. Piper, J. P. Robinson and D. Y. Jin, *Nat. Photonics*, 2014, **8**, 33–37.
21 Z. J. Yang, H. Liu, C. Zong, F. Yan and H. X. Ju, *Anal. Chem.*, 2009, **81**, 5484–5489.
22 Z. F. Fu, H. Liu and H. X. Ju, *Anal. Chem.*, 2006, **78**, 6999–7005.
23 T. Takayanagi, Y. Inaba, H. Kanzaki, Y. Jyoichi and S. Motomizu, *Talanta*, 2009, **79**, 1089–1093.
24 K. C. Ahn, P. Lohstroh, S. J. Gee, N. A. Gee, B. Lasley and B. D. Hammock, *Anal. Chem.*, 2007, **79**, 8883–8890.
25 Y. Q. Lai, Y. Y. Qi, J. Wang and G. N. Chen, *Analyst*, 2009, **134**, 131–137.
26 M. G. Azam, T. Shibata, T. Kabashima and M. Kai, *Anal. Bioanal. Chem.*, 2011, **401**, 1211–1217.
27 F. Bolletta and V. Balzani, *J. Am. Chem. Soc.*, 1982, **104**, 4250–4251.
28 R. Nagao, M. Yokono, A. Teshigahara, S. Akimoto and T. Tomo, *J. Phys. Chem. B*, 2014, **118**, 5093–5100.
29 W. D. Comar, S. M. Schubert, B. Jastrzebska, K. Palczewski and A. W. Smith, *J. Am. Chem. Soc.*, 2014, **136**, 8342–8349.
30 A. Natrajan, D. Sharpe, J. Costello and Q. P. Jiang, *Anal. Biochem.*, 2010, **406**, 204–213.
31 Q. F. Xu, J. Liu, Z. K. He and S. Yang, *Chem. Commun.*, 2010, **46**, 8800–8802.
32 A. Natrajan and D. Wen, *RSC Adv.*, 2013, **3**, 21398–21404.
33 Y. He, G. M. Huang and H. Cui, *ACS Appl. Mater. Interfaces*, 2013, **5**, 11336–11340.

